Small molecule NF-κB inhibitors as immune potentiators for enhancement of vaccine adjuvants

Authors

Brittany A. Moser, Yoseline Escalante-Buendia, Rachel C. Steinhardt, Matthew G. Rosenberger, Britteny J. Cassaidy, Nihesh Naorem, Alfred C. Chon, Minh Nguyen, Ngoctran Tran, Aaron P. Esser-Kahn

Abstract

Adjuvants are added to vaccines to enhance the immune response and provide increased protection against disease. In the last decade, hundreds of synthetic immune adjuvants have been created, but many induce undesirable levels of proinflammatory cytokines including TNF-α and IL-6. Here we present small molecule NF-κB inhibitors that can be used in combination with an immune adjuvant to both decrease markers associated with poor tolerability and improve the protective response of vaccination. Additionally, we synthesize a library of honokiol derivatives identifying several promising candidates for use in vaccine formulations.

Introduction

Vaccines remain one of the most effective ways of preventing disease. Despite their immense success in preventing diseases such as polio, tetanus, and small pox, diseases such as HIV and dengue present challenges that current clinical vaccine technologies cannot provide. To solve this problem, one strategy that has been explored is to include adjuvants, molecules that enhance the immune response.[1] Although novel adjuvants generate higher quality immune responses that cannot be achieved with current approved adjuvants, to date, very few have been approved for use in human vaccines. This disconnect is due, in part, to the challenge of balancing

the proinflammatory immune response with the protective, adaptive immune response.[2–4] We recently reported that vaccines could be improved through the use of a peptide NF-κB inhibitor, SN50 in combination with an immune adjuvant.[5] The addition of SN50 to adjuvanted vaccines led to increased safety of the adjuvant while enhancing protection against disease. Although this method proved both general across a wide range of adjuvants and effective against antigens of a variety of diseases, it still required a large amount of the peptide to enable optimal safety and protection. Scale-up of peptides present synthetic challenges and can result in expensive production costs, limiting their potential in a clinical setting.[6,7] Peptides might also induce an immune response against themselves leading to a potential for decreased enhancement in subsequent vaccinations. We chose to explore other small molecule NF-κB inhibitors as immune potentiators to overcome these challenges.

Here we demonstrate that select small molecule NF-κB inhibitors are effective at reducing adjuvant-induced inflammation while also increasing the adaptive immune response. At the same time, we demonstrate that not all NF-κB inhibitors are effective immune potentiators. Of the molecules we tested, honokiol and capsaicin proved to be effective at both limiting inflammation and potentiating the protective response. Through knockout studies, we demonstrate that the increase in antigen specific antibodies is independent from the anti-inflammatory activity, which is congruent with our previous studies[5]. To determine if these small molecules could be improved by chemical synthesis, we explored derivatives of honokiol and found several promising candidates for potential use in vaccines.

Results and discussion

Exploration of small molecule NF-κB inhibitors *in vitro*

To begin exploring alternative NF-κB inhibitors, we examined the literature for promising candidates. Due to the strong correlation between NF-κB activation and sepsis[8], cancer[9,10] and autoimmune disorders[11], a large library of NF-κB inhibitors have been identified.[12] We first wanted to analyze the potential of a variety small molecule NF-κB inhibitors to inhibit inflammation *in vitro* in combination with lipopolysaccharide (LPS), a TLR4 agonist. We chose several common commercially available NF-κB inhibitors and tested them in RAW macrophages. We chose to examine: Cardamonin (40 μM), Caffeic acid phenethyl ester (CAPE) (100 μM), Withaferin A (WA) (400 nM), Resveratrol (10 μM), Salicin (100 nM), 5Z-7-Oxozeaenol (5-z-O) (5 μM), Parthenolide (20 μM), Honokiol (20 μM), Capsaicin (200 μM), PDK1/Akt/Flt dual pathway inhibitor (PDK1) (1 μM), and GYY 4137 (GYY) (200 μM). To determine if immune potentiation was specific to NF-κB or general to all anti-inflammatory molecules, we included the most common, FDA approved anti-inflammatory drugs acetaminophen (10 mM) and ibuprofen (800 μM).[13,14] We treated RAW macrophages with inhibitors and LPS and assayed the supernatant for IL-6 secretion (**Fig. 1a**).

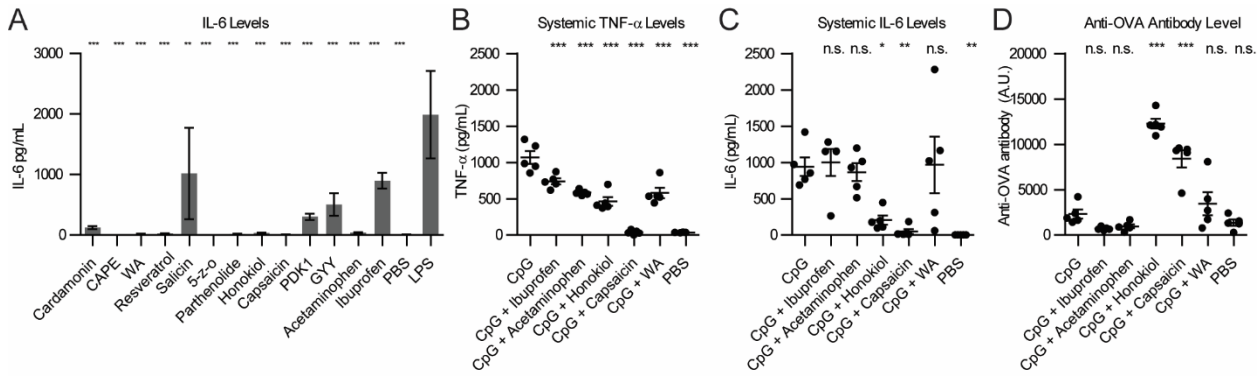

Figure 1. Small molecule inhibitor screen *in vitro* and *in vivo*. (A) IL-6 levels from RAW macrophages 24h post-stimulation with NF-κB inhibitor and LPS. Significance is compared to LPS alone. (B) Systemic TNF- α expression 1h post-vaccination. (C) Systemic IL-6 expression 1h post-vaccination. (D) Anti-OVA antibody level 21 days post-vaccination. Significance is compared to CpG vaccination. * $p < 0.05$, ** $p < 0.01$, $p < 0.001$.

Exploration of small molecule NF-κB inhibitors *in vivo*

We next wanted to examine how these inhibitors would alter safety and protection *in vivo*. To test this *in vivo*, we chose the small molecule inhibitors that were the most effective at inhibiting IL-6 expression *in vitro*, capsaicin, honokiol and withaferin A (WA) and ran them alongside acetaminophen and ibuprofen. We chose to vaccinate mice using CpG, a TLR9 agonist. For our *in vivo* vaccination, we used ovalbumin (OVA) as a model antigen to examine the changes in humoral response. We vaccinated mice with 100 μg OVA, 50 μg CpG, and inhibitor (800 μg ibuprofen, 2 mg acetaminophen, 400 μg honokiol, 20 μg capsaicin or 600 μg WA). Due to the difficulty in solubility, all inhibitors were suspended in Addavax, a squalene-based oil-in-water nano-emulsion, to enable effective vaccine suspensions. We chose to analyze systemic levels of TNF-α and IL-6 because high levels of these cytokines are pyrogenic and have been correlated with undesirable vaccine-related side effects.[15–17] We previously determined that CpG-induced TNF-α and IL-6 peak at 1 h post-vaccination.[5] Mice vaccinated with CpG demonstrated high levels of TNF-α (1067 pg/mL) (**Fig. 1b**). Addition of an NF-κB inhibitor decreased the level of TNF-α. Ibuprofen decreased to the level to 738 pg/mL (1.4 fold), acetaminophen (1.8 fold), honokiol (2.3 fold), capsaicin (28 fold, equivalent to background levels), and WA by 1.8 fold. The systemic levels of IL-6 were also high with CpG vaccination (941 pg/mL). The groups that included an NF-κB inhibitor did not always decrease the level of IL-6 (**Fig. 1c**). Ibuprofen, acetaminophen and WA did not decrease IL-6 expression significantly. However, honokiol and capsaicin dramatically reduced the systemic levels of IL-6 to 266 pg/mL (3.5 fold) and 47.4 pg/mL (20 fold), respectively.

On day 21, we analyzed the anti-OVA antibody levels (**Fig. 1d**). CpG was 1.3 fold higher than PBS. Ibuprofen and acetaminophen were 3.2 and 2.4 fold lower that CpG alone. CpG +

honokiol was 5.3 fold more than CpG alone. CpG + capsaicin was 3.5 fold higher than CpG alone. CpG + WA was 1.5 fold lower than CpG alone.

Dose-dependence of capsaicin and honokiol

Of the candidates, Capsaicin and honokiol demonstrated exceptional promise in these studies so we examined them further. To better understand how these molecules are altering the immune response over time, we vaccinated mice as described above and analyzed a larger variety of cytokines at various. We analyzed 13 cytokines: IL-1α, IL-1β, IL-6, IL-10, IL-12p70, IL-17A, IL-23, IL-27, MCP-1, IFN-β, IFN-γ, TNF-α, and GM-CSF. Of these, only 6 cytokines demonstrated detectable levels in our assay: TNF-α, IL-6, IL-10, IL-1α, MCP-1 and IFN-γ (**Fig. 2a-f**). Consistent with our previous findings[5], CpG induced TNF-α and IL-6 expression peaked at 1 h. Interestingly, CpG combined with either capsaicin or honokiol had increased IFN-γ levels at 24 h compared to CpG alone (8 fold and 9 fold, respectively) and slightly elevated MCP-1 levels (2.5 and 2 fold, respectively), demonstrating that both capsaicin and honokiol are acting to potentiate the immune response and are not simply suppressing immune activation. We next wanted to understand how changing the dose would alter innate and adaptive immune responses. For honokiol, we tested a concentration 2-fold higher (800 μg) and 2- fold lower (200 μg) than the original dose (400 μg). A pain response was observed in mice vaccinated with our original dose of capsaicin (20 μg), so we wanted to examine if we could lower the dose, but maintain adequate anti-inflammatory activity and antibody-boosting potential. We chose to test a dose 4- fold lower (5 μg) and 20- fold lower (1 μg) than the original dose (20 μg). All doses of honokiol demonstrated a significant decrease in TNF-α expression compared to CpG alone, however there was no significant difference between the different doses (**Fig. 2g**). Capsaicin decreased TNF- α levels significantly across all doses compared to CpG alone. Capsaicin doses of 5 μg and 20 μg decreased

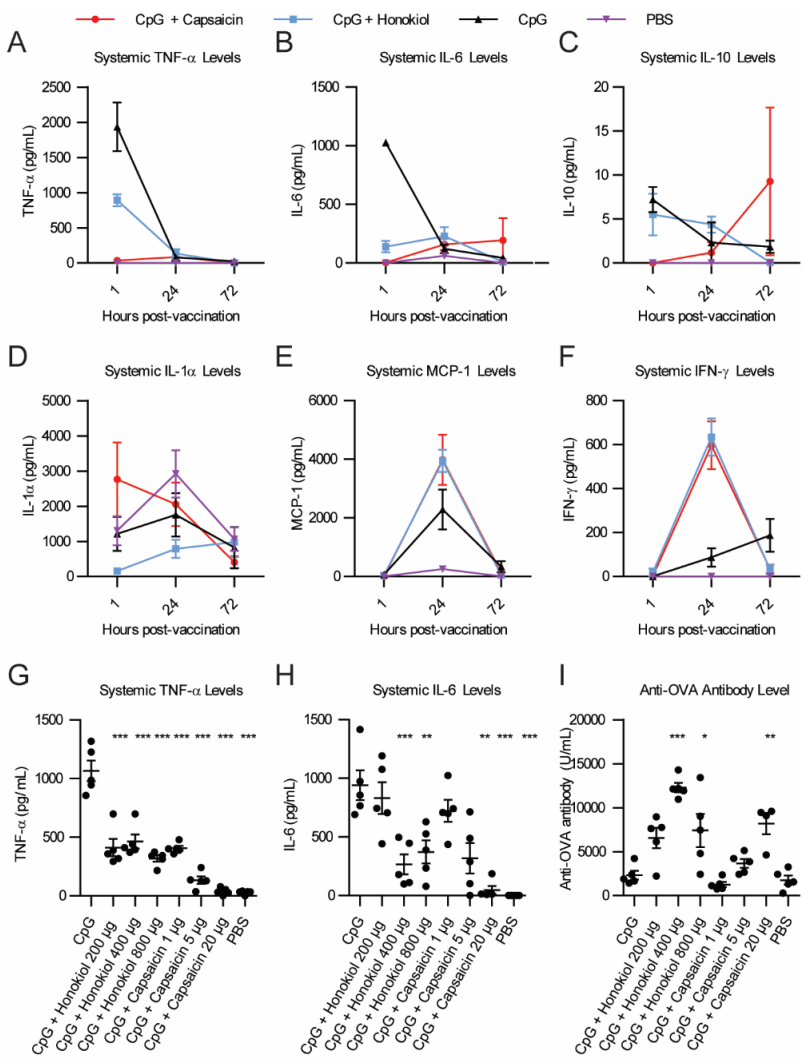

Figure 2. Broader cytokine response and dose effects of honokiol and capsaicin. (A-F) Systemic cytokine levels at 1 h, 24 h and 48 h post-vaccination. CpG (black line), CpG + Capsaicin (red line), CpG + Honokiol (blue line), PBS (purple line) (G) Systemic TNF-α levels 1h post-vaccination with varying doses of honokiol and capsaicin (H) Systemic IL-6 levels 1h post-vaccination (C) Anti-OVA antibody levels 21 days post-vaccination. Significance is compared to CpG alone. * $p < 0.05$, **$p < 0.01$, $p < 0.001$.

levels of TNF-α significantly more than 1 µg (**Fig. 2g**). The level of IL-6 was only decreased with 400 µg and 800 µg honokiol and 20 µg capsaicin (**Fig. 2h**). Twenty-one days later, we analyzed differences in anti-OVA antibody level and found that all doses of honokiol increased levels of anti-OVA antibodies compared to CpG alone and the highest level was found with 400 µg honokiol (**Fig. 2i**). 1 µg and 5 µg of capsaicin did not change level of anti-OVA antibodies in the serum compared to CpG alone, however 20 µg significantly increased serum levels.

Determining the TRPV1-mediated effects of capsaicin

The primary in vivo target for capsaicin is the transient receptor potential cation channel subfamily V member 1 (TRPV1). TRPV1 modulates the immune response in a variety of ways, and importantly, has been implicated in dampening systemic inflammation associated with

sepsis.[18–22] However, it has never been explored in a vaccine setting. To understand how activation of TRPV1 may be modulating the effects of the adjuvant, we compared the immediate inflammatory response of the vaccination in wild type mice (WT) and TRPV1 knockout mice. We vaccinated WT and TRPV1 KO mice with 100 μg OVA and: 50 μg CpG, 50 μg CpG + 20 μg capsaicin or PBS. We analyzed systemic levels of TNF-α and IL-6 1 h after vaccination. We found that CpG induced high levels of TNF-α and IL-6 in both WT and TRPV1 KO mice. Addition of capsaicin dramatically and significantly reduced both TNF-α levels and IL-6 levels in the WT mice (**Fig. 3a, 3b, S1**). Although the mean was slightly lower for both TNF-α and IL-6 in the TRPV1 KO mice, these differences were not statistically significant. This demonstrated that TRPV1 activation is responsible for the capsaicin-induced decrease in systemic cytokine levels. To examine if the increased antibody level was due to TRPV1 activation on day 21, we analyzed levels of anti-OVA antibodies in the serum (**Fig. 3c, S1**). Interestingly, we found that anti-OVA antibody levels were increased in groups with Capsaicin + CpG in both WT and KO mice. This implies that the antibody-boosting activity of capsaicin is separate from TRPV1-dependent decrease in inflammatory cytokines. This result demonstrates both that the decrease in inflammation is not responsible for the antibody-boosting activity of the NF-κB inhibitor and also that the enhancement of the adaptive response is independent of TRPV1 activation. These results, while not definitive, showed two separate, but correlated mechanisms for capsaicin that result in the reduction in cytokines and increase antibody levels. As such, capsaicin did not warrant further examination as a potential clinical immune potentiator. We will explore the mechanistic implications of this for immune potentiators more broadly in future publications.

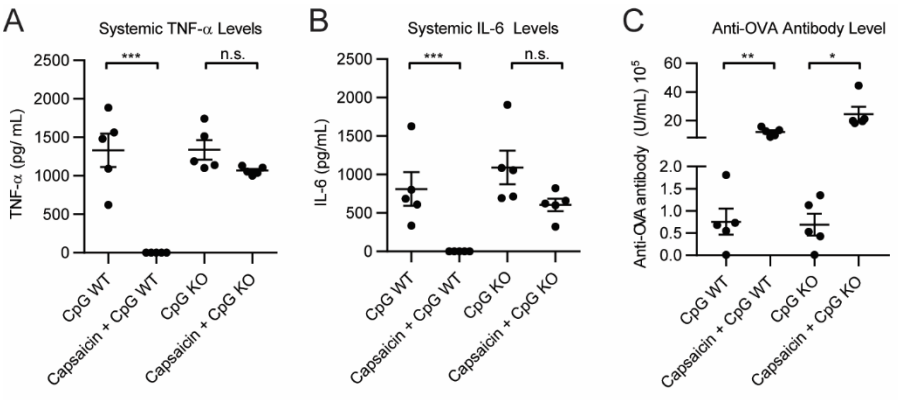

Figure 3. Role of TRPV1 of capsaicin induced anti-inflammatory and immune potentiation. (A) Systemic TNF-α levels 1 h post vaccination in wild type (WT) mice and TRPV1 KO (KO). (B) Systemic IL-6 levels 1 h post-vaccination. (C) Anti-OVA antibody level 21 days post-vaccination. * $p < 0.05$, **$p < 0.01$, $p < 0.001$.

Synthesis of honokiol derivative library

With capsaicin possessing two parallel mechanisms and possessing well-established side effects[23], we wanted to explore honokiol for further development as a candidate. An important question for immune potentiators and honokiol was if standard SAR methods would yield alteration in potentiation activity. To further explore this idea, we synthesized a library of derivatives. Honokiol derivative libraries have been synthesized previously and examined for their effects on neuroprotection[24], antimicrobial agents[25] and anti-cancer[26] among others.[27,28] However, to date no such study has examined the effects of honokiol analogs on vaccines or a combination of anti-inflammatory activity and adaptive immune response. Phenylphenols and biphenols were prepared using Pd-catalyzed Suzuki coupling using corresponding iodophenols and hydroxyphenylboronoic acids as starting materials. These compounds were *O*-allylated using allylBr. Resulting compounds were subjected to Claisen rearrangement using diethyl aluminum chloride to yield a variety of ring substitutions (**Scheme 1, Fig. 4a**).

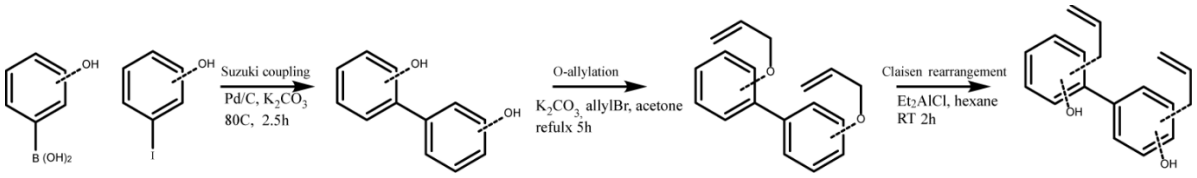

Scheme 1. Honokiol derivative synthesis.

We analyzed how the honokiol derivatives altered IL-6 production in RAW macrophages. We chose to analyze the hydroxybiphenyls and *O*-allylated derivatives in addition to the product from the Claisen rearrangement to understand how these functional groups play a role in the anti-inflammatory action or increase in adaptive immune response (**Fig. 4b, S2, S3**). We treated RAW macrophages with honokiol derivatives and LPS and analyzed IL-6 expression. The addition of LPS alone without a honokiol derivative gave high levels of IL-6 expression (6848 pg/mL). The addition of honokiol decreased IL-6 levels to 260 pg/mL, a decrease of 26-fold. Several derivatives including compounds: **1**, **2**, **3**, **4**, **8**, and **11** demonstrated similar reductions in IL-6 expression.

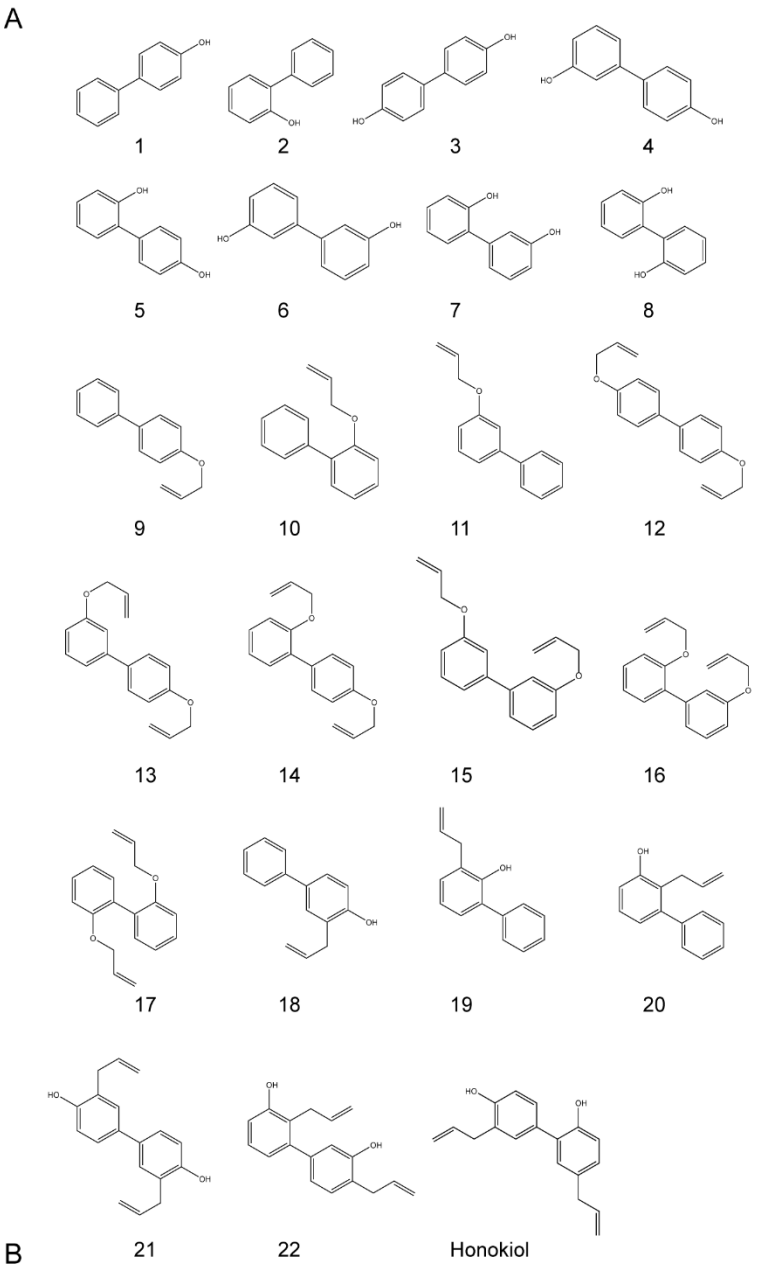

Figure 4. Honokiol derivatives and their inhibitory activity on IL-6 expression. (A) Honokiol derivative library (B) IL-6 expression of RAW macrophages treated with honokiol derivatives and LPS. Significance is compared to LPS alone. * $p < 0.05$, **$p < 0.01$, $p < 0.001$.

Conclusion

In summary, we present that select small molecule inhibitors of NF-κB can decrease the inflammatory effects of adjuvanted vaccination - potentially enabling safer vaccination while also acting as immune potentiators and increasing the antibody level. We identified two such immune potentiators, honokiol and capsaicin that effectively decrease inflammation while increasing the adaptive response. We additionally provide evidence that implies that the decrease in inflammation is separate from the increase in antibody response, potentially enabling distinct tunability of either response. This study also identifies that only select NF-κB inhibitors can be used as immune potentiators, this broadens the potential for further modulation of the immune response. We additionally synthesized and examined a library of honokiol derivatives and found that several honokiol derivatives are promising candidates for future testing *in vivo*. In conclusion, we have demonstrated that using small molecule NF-κB inhibitors in combination with common immune adjuvants can decrease the production of pro-inflammatory cytokines TNF-α and IL-6 while boosting antibody levels.

Materials and methods

In vitro assays

RAW macrophage cytokine analysis

RAW 264.7 macrophages were passaged and plated in a cell culture treated 12- well plate at 0.5 $x10^6$ cells/ well in 1 mL DMEM containing 10% FBS. Cells were grown for 2 days. Media was exchanged for 1 mL DMEM containing 10% HIFBS. Inhibitors were diluted in Addavax and then

in PBS. Inhibitors were added at indicated concentrations and incubated for 45 min. After 45 min, LPS was added at 100 ng/mL and incubated at 37 °C and 5% CO_2 for 24 h. Cell supernatant was removed and analyzed using BD Cytometric Bead Array Mouse Inflammation Kit.

Cell viability assay

RAW macrophages were plated at 100k cells/ well in 180 uL DMEM/10% HIFBS. Inhibitors were diluted as described above and added at indicated concentrations and incubated for 45 min. After 45 min, LPS was added to a final concentration of 100 ng/mL and incubated at 37 °C and 5% CO_2 for 24 h. MTT reagent was made fresh at a concentration of 5 mg/mL in PBS and sterile filtered. 150 μL cell supernatant was removed and 150 μL PBS was added. 10 μL MTT reagent was added to each well and incubated at 37 °C and 5% CO_2 for 2 h. 150 μL supernatant was removed from each well and replaced with 150 μL DMSO and incubated at 37 °C and 5% CO_2 for 1 h or until purple crystals dissolved. Plate was analyzed using Multiskan FC plate reader (Thermo Scientific) and absorbance was measured at 450 nm. Data was analyzed using Graphpad Prism.

Flow cytometry

RAW macrophages (2×10^6) were plated in a 12 well plate in DMEM/10% HIFBS. Inhibitors were diluted as described above and added at indicated concentrations and incubated for 45 min. After 45 min, LPS was added to a final concentration of 100 ng/mL and incubated at 37 °C and 5% CO_2 for 24 h. Cells were stained for CD86 using BD cytofix/cytoperm fixation /permeabilization solution kit according to manufacter's protocol. Cells were analyzed using NovoCyte flow cytometer (ACEA Biosciences, Inc.).

In vivo assays

All animal procedures were performed under a protocol approved by the University of Chicago Institutional Animal Care and Use Committee (IACUC). 6-8 week-old C57/B6 female mice were purchased from Jackson Laboratory (JAX). 6-8 week-old C57/B6 female Trpv1^{tm1Ju} mice were purchased from JAX for TRPV1 KO experiment. All compounds were tested for endotoxin prior to use. All vaccinations were administered intramuscularly in the hind leg. Blood was collected from the sapheneous vein at time points indicated.

Antigens were purchased from Invitrogen (Vaccigrade Ovalbumin). Vaccigrade CpG ODN 1826 was purchased from Adipogen. AddaVax™ was purchased from Invivogen.

Vaccination

Mice were lightly anesthetized with isoflurane and injected intramuscularly in the hind leg with 50 µL containing ovalbumin (100 µg), adjuvant, inhibitor and PBS. Adjuvant doses: CpG, 50 µg. Inhibitor concentrations: Honokiol (400 µg), Capsaicin (20 µg), Withaferin A (600 µg), acetaminophen (2 mg), ibuprofen (800 µg). All vaccines contained 25 µL AddaVax™ to enhance solubility.

Plasma cytokine analysis

Blood was collected from mice at time points indicated in 0.2 mL heparin coated collection tubes (VWR Scientific). Serum was isolated via centrifugation 2000 x g for 5 min. Supernatant was collected and stored at -80 °C until use. Serum was analyzed using BD Cytometric Bead Array Mouse Inflammation cytokine kit or LEGENDplex™ Mouse Inflammation Panel (Biolegend) according to manufacturer's protocol.

Antibody quantification

Mice were vaccinated with indicated formulations. Blood was collected at time points indicated in 0.2 mL heparin coated collection tubes (VWR Scientific) for plasma or uncoated tubes for serum. Plasma was isolated via centrifugation (2000 x g, 5 min). Serum was isolated by allowing blood to clot for 15- 30 min RT and centrifuging (2000 x g for 10 min) at 4 °C. Serum was analyzed using a quantitative anti-ovalbumin total Ig's ELISA kit (Alpha Diagnostic International) according to the specified protocol. Data was analyzed using Graphpad Prism.

Chemistry

Conditions for Suzuki Coupling

Hydroxyphenol boronic acid (20 mmol) was dissolved in 100 mL water. Appropriate iodophenol (10 mmol) and K_2CO_3 (40 mmol) was added followed by Pd/C (2 mol %). Solution heated to 80 C for 3h. Solution was acidified with 1M HCl and extracted with EtoAc and washed with brine. Solvent evaporated in vacuo. Compound was purified by column chromatography.

1, **2**, **3**, **8** were purchased from Sigma Aldrich.

(4): Spectral data as previously described: Schmidt, B.; Riemer, M., Journal of Organic Chemistry, 2014, 4104 – 4118.

^{1}H NMR (400 MHz, $CDCl_3$) δ 7.54 – 7.38 (m, 2H), 7.37 – 7.27 (m, 1H), 7.10 (ddd, *J* = 7.7, 1.7, 1.0 Hz, 1H), 7.08 – 6.96 (m, 1H), 6.93 – 6.85 (m, 2H), 6.82 – 6.73 (m, 1H).

HRMS (ESI) calculated for C24H18O3 [2M-H_2O]+: 354.1256, found: 354.1259.

(5): Spectral data as previously described: Reddy, B.V.S; Rao, R.N.; Reddy, N.S.S.; Somaiah, R.; Yadav, J.S.; Subramanyam, R., Tetrahedron Letters, 2014, 1049 – 1051.

^{1} H NMR (400 MHz, $CDCl_3$) δ 7.35 (d, *J* = 8.6 Hz, 2H), 7.25 – 7.18 (m, 2H), 7.03 – 6.93 (m, 4H).

HRMS (ESI) calculated for C18H19O2 [M+H]+: 267.1385, found: 267.1400.

(6): Spectral data as previously described: Moorthy, J. ; Venkatakrishnan, P.; Samanta, S., Organic and Biomolecular Chemistry, 2007, 1354 – 1357.

^{1}H NMR (400 MHz, $CDCl_3$) δ 7.30 (t, *J* = 7.9 Hz, 2H), 7.14 (ddd, *J* = 7.7, 1.7, 1.0 Hz, 2H), 7.04 (dd, *J* = 2.5, 1.6 Hz, 2H), 6.82 (ddd, *J* = 8.1, 2.6, 1.0 Hz, 2H).

HRMS (ESI) calculated for C12H9O2 [M-H]-: 185.0603, found: 185.0633.

(7): Spectral data as previously described: Sánchez-Peris, M.; Falomir, E.; Murga, J.; Carda, M.; Marco, J. Bioorganic and Medicinal Chemistry, 2016, 3108 – 3115.

^{1}H NMR (400 MHz, $CDCl_3$) δ 7.30 (t, *J* = 7.9 Hz, 1H), 7.25 – 7.16 (m, 2H), 7.00 – 6.93 (m, 3H), 6.91 (dd, *J* = 2.6, 1.6 Hz, 1H), 6.83 (ddd, *J* = 8.2, 2.6, 1.0 Hz, 1H).

HRMS (ESI) calculated for C12H9O2 [M+H]-: 185.0603, found: 185.0635.

Conditions for O-allylations

Phenol (1 mmol) (Derivative **1**-**8**) was dissolved in dry acetone (5 mL) and K_2CO_3 (2 mmol) added. AllylBr was added dropwise and refluxed. Reaction was monitored by TLC until completion (5-12h). Reaction mixture was cooled and volatiles were removed in vacuo. 10% NaOH was added to the mixture and extraction was performed using ethyl acetate, washed with brine and organic layers dried using $MgSO_4$. Solvent was removed in vacuo affording an oily material that was purified by column chromatography to yield the O-allylated derivative.

(**9**): Spectral data as previously reported: Khan, A.; Komejan, S.; Patel, A.; Lombardi, C.; Lough, A.; Foucher, D., Journal of Organometallic Chemistry, 2015, 180 – 191.

^{1}H NMR (400 MHz, $CDCl_3$) δ 7.54 (ddt, *J* = 11.8, 5.2, 2.2 Hz, 4H), 7.46 – 7.37 (m, 2H), 7.34 – 7.28 (m, 1H), 7.04 – 6.96 (m, 2H), 6.09 (ddt, *J* = 17.2, 10.5, 5.3 Hz, 1H), 5.45

(dq, *J* = 17.3, 1.6 Hz, 1H), 5.31 (dq, *J* = 10.5, 1.4 Hz, 1H), 4.59 (dt, *J* = 5.3, 1.5 Hz, 2H).

HRMS (ESI) calculated for C30H32NO [2M+NH4]+: 438.2471, found: 438.2403.

(10): Spectral data as reported: Bujok, R.; Bieniek, M.; Masnyk, M.; Michrowska, A.; Sarosiek, A.;Stępowska, H.; Arlt, D.; Grela, K. J. Org. Chem. 2004, 69, 6894-6896.

^{1}H NMR (400 MHz, $CDCl_3$) δ 7.58 (dq, *J* = 2.6, 1.7 Hz, 2H), 7.48 – 7.38 (m, 2H), 7.38 –

7.27 (m, 3H), 7.09 – 7.02 (m, 1H), 6.99 (dd, *J* = 8.2, 0.8 Hz, 1H), 6.00 (ddt, *J* = 17.3, 10.6, 4.8 Hz, 1H), 5.34 (dq, *J* = 17.3, 1.7 Hz, 1H), 5.21 (dq, *J* = 10.6, 1.6 Hz, 1H), 4.55 (dt, *J* = 4.8, 1.7 Hz, 2H).

HRMS (ESI) calculated for C15H15O [M+H]+: 211.1127, found: 211.1125.

(**11**): Spectral data as previously reported: Sánchez-Peris, M., Murga, J., Falomir, E., Carda, M., & Marco, J. A. Chemical biology & drug design 2017, 577-584.

^{1}H NMR (400 MHz, $CDCl_3$) δ 7.59 (dt, *J* = 8.4, 2.5 Hz, 2H), 7.43 (dt, *J* = 6.9, 4.8 Hz,

2H), 7.34 (td, *J* = 7.8, 2.2 Hz, 2H), 7.23 – 7.18 (m, 1H), 7.16 (q, *J* = 2.3 Hz, 1H), 6.91 (dd, *J* = 8.2, 2.7 Hz, 1H), 6.09 (dddd, *J* = 15.8, 8.0, 6.6, 4.1 Hz, 1H), 5.45 (dq, *J* = 17.3, 1.6 Hz, 1H), 5.31 (dq, *J* = 10.5, 1.5 Hz, 1H), 4.65 – 4.54 (m, 2H).

HRMS (ESI) calculated for $C_{15}H_{15}O$ [M+H]+: 211.1123, found: 211.1125.

(12): Spectral data as previously reported: Schlosser, M.; Michel, D.; Croft, S. Synthesis 1996, 591-593.

^{1}H NMR (400 MHz, $CDCl_3$) δ 7.49 – 7.44 (m, 4H), 7.03 – 6.90 (m, 4H), 6.08 (ddt, *J* = 17.2, 10.6, 5.3 Hz, 2H), 5.44 (dq, *J* = 17.3, 1.6 Hz, 2H), 5.30 (dq, *J* = 10.5, 1.4 Hz, 2H),

4.57 (dt, *J* = 5.3, 1.5 Hz, 4H).

HRMS (ESI) calculated for C18H19O2 [M+H]+: 267.1394, found: 267.1389.

(13): Spectral data as previously reported: Tripathi, S.; Chan, M; Chen, C. Bioorg. Med. Chem. Lett. 2012, 22, 216-221.

^{1}H NMR (400 MHz, $CDCl_3$) δ 7.56 – 7.48 (m, 2H), 7.32 (t, *J* = 7.9 Hz, 1H), 7.14 (ddd, *J* =

7.7, 1.6, 0.9 Hz, 1H), 7.12 – 7.09 (m, 1H), 7.02 – 6.94 (m, 2H), 6.86 (ddd, *J* = 8.2, 2.6, 0.9 Hz, 1H), 6.21 – 6.02 (m, 2H), 5.44 (ddd, *J* = 17.3, 3.1, 1.5 Hz, 2H), 5.34 – 5.26 (m, 2H), 4.64 – 4.55 (m, 4H).

HRMS (ESI) calculated for C18H19O2 [M+H]+: 267.1394, found: 267.1391.

(14): Spectral data as previously reported: Reddy, B.V.S; Rao, R.N.; Reddy, N.S.S.; Somaiah, R.; Yadav, J.S.; Subramanyam, R., Tetrahedron Letters, 2014, 1049 – 1051.

^{1}H, 500 MHz): δ 7.39 (d, J = 9.0 Hz, 2H), 7.14-7.21 (m, 2H), 6.86-6.90 (m, 4H), 5.87-5.97 (m, 2H), 5.08-5.32 (m, 4H), 4.46 (d, J = 5Hz, 2H), 4.41 (d, J = 5Hz, 2H)

HRMS (ESI) calculated for $C_{18}H_{18}O_2$ [M+H]+: 266.1307, found: 266.1316.

(15): Spectral data as previously reported: Sánchez-Peris, M., Murga, J., Falomir, E., Carda, M., & Marco, J. A. Chemical biology & drug design 2017, 577-584.

^{1}H NMR (400 MHz, $CDCl_3$) δ 7.36 (t, *J* = 7.9 Hz, 2H), 7.20 (ddd, *J* = 7.6, 1.7, 1.0 Hz,

2H), 7.17 (dd, *J* = 2.6, 1.6 Hz, 2H), 6.93 (ddd, *J* = 8.2, 2.5, 1.0 Hz, 2H), 6.11 (ddt, *J* = 17.3, 10.5, 5.3 Hz, 2H), 5.47 (dq, *J* = 17.3, 1.6 Hz, 2H), 5.33 (dq, *J* = 10.5, 1.4 Hz, 2H),

4.62 (dt, *J* = 5.3, 1.6 Hz, 4H).

HRMS (ESI) calculated for $C_{18}H_{18}O_2$ [M+H]+: 267.1385, found: 267.1386.

(16): Spectral data as previously reported: Sánchez-Peris, M., Murga, J., Falomir, E., Carda, M., & Marco, J. A. Chemical biology & drug design 2017, 577-584.

^{1}H NMR (400 MHz, $CDCl_3$) δ 7.38 – 7.33 (m, 1H), 7.33 – 7.27 (m, 2H), 7.16 (ddd, *J* =

5.3, 2.7, 1.4 Hz, 2H), 7.04 (td, *J* = 7.5, 1.1 Hz, 1H), 6.98 (dd, *J* = 8.3, 1.1 Hz, 1H), 6.90 (ddd, *J* = 8.2, 2.6, 1.1 Hz, 1H), 6.17 – 5.92 (m, 2H), 5.39 (ddq, *J* = 35.8, 17.3, 1.7 Hz, 2H), 5.26 (ddq, *J* = 30.6, 10.6, 1.5 Hz, 2H), 4.56 (ddt, *J* = 10.4, 4.9, 1.6 Hz, 4H).

HRMS (ESI) calculated for C18H19O2 [M+H]+: 267.1394, found: 267.1395.

(17): Spectral data as previously reported: Sánchez-Peris, M., Murga, J., Falomir, E., Carda, M., & Marco, J. A. Chemical biology & drug design 2017, 577-584.

^{1}H NMR (400 MHz, $CDCl_3$) δ 7.29 (dtd, *J* = 8.2, 7.2, 3.8 Hz, 4H), 7.09 – 6.99 (m, 2H),

6.95 (d, *J* = 8.2 Hz, 2H), 5.92 (ddt, *J* = 17.3, 10.6, 4.8 Hz, 2H), 5.22 (ddd, *J* = 17.3, 3.5, 1.8 Hz, 4H), 5.13 (ddd, *J* = 10.6, 3.2, 1.6 Hz, 4H), 4.51 (dt, *J* = 4.6, 1.7 Hz, 4H).

HRMS (ESI) calculated for $C_{18}H_{18}O_2$ [M+H]+: 267.1385, found: 267.1380.

Conditions for Claisen rearrangement

O-allylated derivatives (**9**-**17**) (1 mmol) were dissolved in dry hexane (10 mL). Et_2AlCl in dry hexane (4 mL) was added dropwise under argon. Mixture was stirred at room temperature for 2h. The mixture was cooled on an ice bath and quenched using 2M HCl (20 mL). Extraction was performed with EtOAc, washed with brine and dried over MgSO4. Solvent was removed in vacuo affording an oily material that was purified by column chromatography to yield the C-allyl derivative.

(18): Spectral data as previously reported: Sánchez-Peris, M., Murga, J., Falomir, E., Carda, M., & Marco, J. A. Chemical biology & drug design 2017, 577-584.

^{1}H NMR (400 MHz, $CDCl_3$) δ 7.60 – 7.51 (m, 2H), 7.47 – 7.34 (m, 5H), 7.34 – 7.27 (m, 1H), 6.89 (d, *J* = 8.1 Hz, 1H), 6.06 (ddt, *J* = 17.2, 10.1, 6.4 Hz, 1H), 5.26 – 5.16 (m, 2H), 3.49 – 3.46 (m, 2H).

HRMS (ESI) calculated for C18H19O2 [M+H]+: 267.1394, found: 267.1381.

(19): Spectral data as previously reported: Sánchez-Peris, M., Murga, J., Falomir, E., Carda, M., & Marco, J. A. Chemical biology & drug design 2017, 577-584.

^{1}H NMR (400 MHz, $CDCl_3$) δ 7.54 – 7.44 (m, 5H), 7.43 – 7.35 (m, 1H), 7.14 (ddd, *J* =

9.3, 4.6, 1.1 Hz, 2H), 6.95 (t, *J* = 7.5 Hz, 1H), 6.07 (ddt, *J* = 16.6, 10.0, 6.6 Hz, 1H), 5.14 (qdd, *J* = 3.2, 2.6, 1.5 Hz, 2H), 3.48 (d, *J* = 6.6 Hz, 2H).

HRMS (ESI) calculated for C15H15O [2M+H]+: 421.2168, found: 421.2173.

(20): Spectral data as previously reported: Eisai R&D Management Co., Ltd. - EP1847535A1, **2007**.

^{1}H NMR (400 MHz, $CDCl_3$) δ 7.60 – 7.54 (m, 1H), 7.48 – 7.28 (m, 4H), 7.23 – 7.16 (m,

1H), 7.14 (dd, *J* = 7.8, 1.8 Hz, 0H), 7.07 (d, *J* = 1.7 Hz, 0H), 6.92 – 6.86 (m, 1H), 6.17 – 5.91 (m, 1H), 5.26 – 5.06 (m, 2H), 3.46 (dt, *J* = 6.4, 1.7 Hz, 1H), 3.35 (dt, *J* = 5.6, 1.9 Hz, 1H).

HRMS (ESI) calculated for $C_{15}H_{15}O$ [M+H]+: 211.1123, found: 211.1125.

***(*21):** Spectral data as previously reported: M.-Y. Chang, S.-Y. Lin, C.-K. Chan, Tetrahedron 2013, 69, 2933-2940.

^{1}H NMR (400 MHz, $CDCl_3$) δ 7.38 – 7.22 (m, 4H), 6.87 (t, *J* = 10.0 Hz, 2H), 6.06 (ddt, *J* = 16.5, 10.1, 6.3 Hz, 2H), 5.28 – 5.12 (m, 4H), 3.47 (d, *J* = 6.3 Hz, 4H).

HRMS (ESI) calculated for C18H19O2 [M+H]+: 267.1394, found: 267.1408.

(22): Spectral data as previously reported: Sánchez-Peris, M., Murga, J., Falomir, E., Carda, M., & Marco, J. A. Chemical biology & drug design 2017, 577-584.

^{1}H NMR (400 MHz, $CDCl_3$) δ 7.21 – 7.00 (m, 3H), 6.91 – 6.66 (m, 3H), 6.16 – 5.78 (m, 2H), 5.25 – 4.88 (m, 4H), 3.54 – 3.32 (m, 4H).

HRMS (ESI) calculated for $C_{18}H_{18}O_2$ [M+H]+: 267.1385, found: 267.1390.

Funding: We would like to acknowledge support by the NIH (1U01Al124286-01 and 1DP2Al112194-01, GM099594). Prof. Esser-Kahn thanks the Pew Scholars Program and the Cottrell Scholars Program for generous support. B.A.M. thanks NSF-GRFP (DGE-1321846). We would like to thank NSF instrumentation grant CHE-1048528. This work was supported, in part, by a grant from the Alfred P. Sloan foundation.

Author contributions: B.A.M. and A.E.K. conceived of and designed the project and experiments and wrote the manuscript. B.A.M., Y.E.B, R.C.S., M.G.R., B.J.C., M.N., N.T. performed experiments. B.A.M. synthesized materials. B.A.M., N.N., A.C.C. performed compound

characterization. Competing interests: The authors report no competing interests. Data and materials availability: All data are available in the main text or the supplementary materials.

References

1. Coffman, R. L., Sher, A. & Seder, R. A. Vaccine adjuvants: putting innate immunity to work. *Immunity* **33**, 492–503 (2010).
2. Audibert, F. M. & Lise, L. D. Adjuvants: current status, clinical perspectives and future prospects. *Trends in Pharmacological Sciences* **14**, 174–178 (1993).
3. Bhardwaj, N., Gnjatic, S. & Sawhney, N. B. TLR AGONISTS: Are They Good Adjuvants? *Cancer J* **16**, 382–391 (2010).
4. Tom, J. K. *et al.* Applications of Immunomodulatory Immune Synergies to Adjuvant Discovery and Vaccine Development. *Trends in Biotechnology* **37**, 373–388 (2019).
5. Moser, B.; Steinhardt, R.; Escalante-Buendia, Y.; Boltz, D.; Barker, K.; Yoo, S.; McGonnigal, B.; Esser-Kahn, A. Immune potentiator for increased safety and improved protection of vaccines by NF-kB modulation. bioRxiv, 2018. doi: https://doi.org/10.1101/4897326.
6. Lau, J. L. & Dunn, M. K. Therapeutic peptides: Historical perspectives, current development trends, and future directions. *Bioorganic & Medicinal Chemistry* **26**, 2700–2707 (2018).
7. Otvos, L. & Wade, J. D. Current challenges in peptide-based drug discovery. *Front Chem* **2**, (2014).
8. Shimaoka, M., & Park, E. J. (2008). Advances in understanding sepsis. European Journal of Anaesthesiology, 25(S42), 146-153.
9. Dolcet, X., Llobet, D., Pallares, J. & Matias-Guiu, X. NF-kB in development and

progression of human cancer. *Virchows Arch* **446**, 475–482 (2005).

10. Xia, Y., Shen, S. & Verma, I. M. NF-κB, an active player in human cancers. *Cancer Immunol Res* **2**, 823–830 (2014).
11. Bacher, S. & Schmitz, M. L. The NF-kB Pathway as a Potential Target for Autoimmune Disease Therapy. (2004). doi:doi/10.2174/1381612043383584
12. Inhibitors of NF-kappaB signaling: 785 and counting. doi:10.1038/sj.onc.1209982
13. Scheuren, N., Bang, H., Münster, T., Brune, K. & Pahl, A. Modulation of transcription factor NF-κB by enantiomers of the nonsteroidal drug ibuprofen. *British Journal of Pharmacology* **123**, 645–652 (1998).
14. Boulares, A. H., Giardina, C., Inan, M. S., Khairallah, E. A. & Cohen, S. D. Acetaminophen inhibits NF-kappaB activation by interfering with the oxidant signal in murine Hepa 1-6 cells. *Toxicol. Sci.* **55**, 370–375 (2000).
15. Christian, L. M., Porter, K., Karlsson, E. & Schultz-Cherry, S. Proinflammatory cytokine responses correspond with subjective side effects after influenza virus vaccination. *Vaccine* **33**, 3360–3366 (2015).
16. Simon, W. L., Salk, H. M., Ovsyannikova, I. G., Kennedy, R. B. & Poland, G. A. Cytokine production associated with smallpox vaccine responses. *Immunotherapy* **6**, 1097–1112 (2014).
17. Netea, M. G., Kullberg, B. J., Meer, V. der & M, J. W. Circulating Cytokines as Mediators of Fever. *Clin Infect Dis* **31**, S178–S184 (2000).
18. Brito, R., Sheth, S., Mukherjea, D., Rybak, L. P. & Ramkumar, V. TRPV1: A Potential Drug Target for Treating Various Diseases. *Cells* **3**, 517–545 (2014).
19. Wang, Y. & Wang, D. H. TRPV1 Ablation Aggravates Inflammatory Responses and Organ

Damage during Endotoxic Shock. *Clin. Vaccine Immunol.* **20**, 1008–1015 (2013).

20. Toledo-Mauriño, J. J. *et al.* The Transient Receptor Potential Vanilloid 1 Is Associated with Active Inflammation in Ulcerative Colitis. *Mediators of Inflammation* (2018). doi:10.1155/2018/6570371
21. Bodkin, J. V. & Fernandes, E. S. TRPV1 and SP: key elements for sepsis outcome? *Br J Pharmacol* **170**, 1279–1292 (2013).
22. Fernandes, E. S. *et al.* TRPV1 deletion enhances local inflammation and accelerates the onset of systemic inflammatory response syndrome. *J. Immunol.* **188**, 5741–5751 (2012).
23. Winter, J. K., Bevan, S. A. & Campbell, E. A. Capsaicin and pain mechanisms. *British journal of anaesthesia* **75**, 157–168 (1995).
24. Tripathi, S., Chan, M.-H. & Chen, C. An expedient synthesis of honokiol and its analogues as potential neuropreventive agents. *Bioorganic & Medicinal Chemistry Letters* **22**, 216–221 (2012).
25. Kim, Y.-S. *et al.* Synthesis and microbiological evaluation of honokiol derivatives as new antimicrobial agents. *Arch. Pharm. Res.* **33**, 61–65 (2010).
26. Sánchez-Peris, M., Murga, J., Falomir, E., Carda, M. & Marco, J. A. Synthesis of honokiol analogues and evaluation of their modulating action on VEGF protein secretion and telomerase-related gene expressions. *Chem Biol Drug Des* **89**, 577–584 (2017).
27. Shen, J.-L. *et al.* Honokiol and magnolol as multifunctional antioxidative molecules for dermatologic disorders. *Molecules* **15**, 6452–6465 (2010).
28. Lee, Y.-J. *et al.* Therapeutic applications of compounds in the Magnolia family. *Pharmacol. Ther.* **130**, 157–176 (2011).

Supplementary Materials for

Small molecule NF-κB inhibitors as immune potentiators for enhancement of vaccine adjuvants

Brittany A. Moser, Yoseline Escalante-Buendia, Rachel C. Steinhardt, Matthew G. Rosenberger, Britteny J. Cassaidy, Nihesh Naorem, Alfred C. Chon, Minh Nguyen, Ngoctran Tran, Aaron P. Esser-Kahn*

*Correspondence to: aesserkahn@uchicago.edu

This PDF file includes:

Figs. S1 to S3

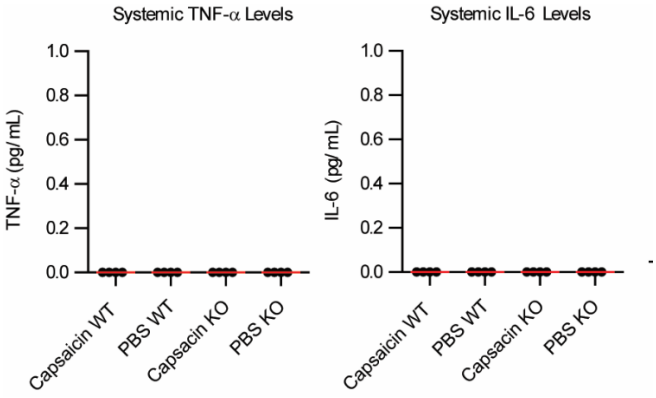

Figure S1. Capsaicin and PBS alone vaccinations in wild type and TRPV1 KO mice.

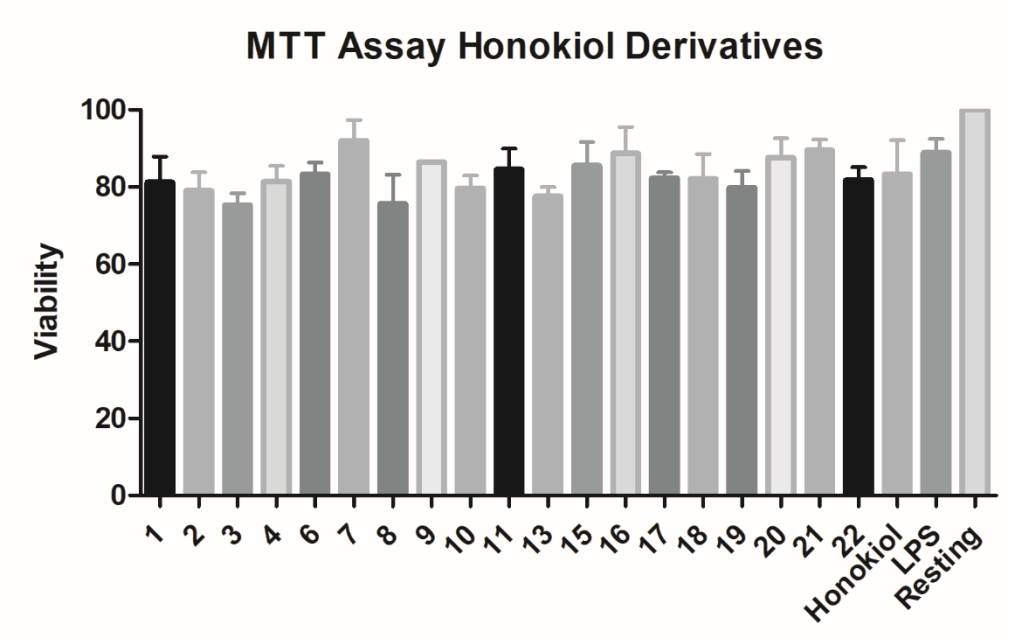

S2. Cell viability of RAW macrophages treated with honokiol derivative library

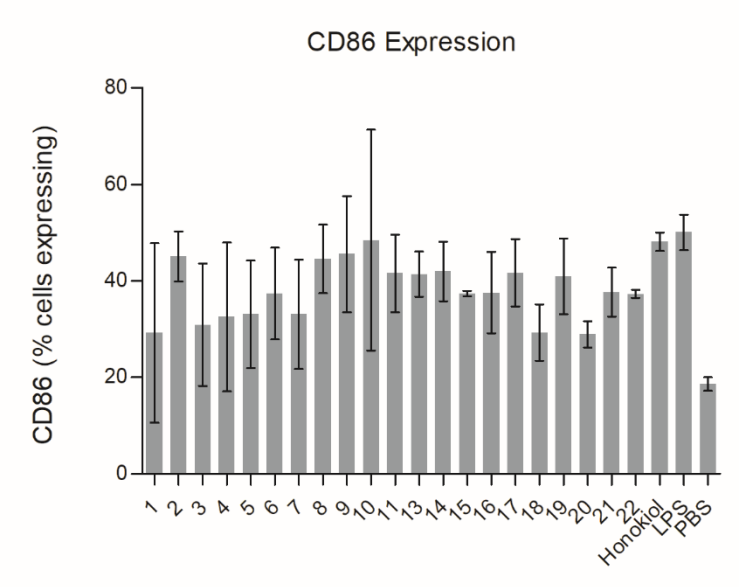

Figure S3. CD86 expression in RAW macrophages